An efficient and accurate approach to modelling the microstructure and defect properties of $LaCoO_3$

J. Buckeridge,[1,*] F. H. Taylor,[1] and C. R. A. Catlow[1]

[1] *University College London, Kathleen Lonsdale Materials Chemistry, Department of Chemistry, 20 Gordon Street, London WC1H 0AJ, United Kingdom*

Complex perovskite oxides are promising materials for cathode layers in solid oxide fuel cells. Such materials have intricate electronic, magnetic and crystalline structures that prove challenging to model accurately. We analyse a wide range of standard density functional theory approaches to modelling a highly promising system, the perovskite $LaCoO_3$, focussing on optimising the Hubbard U parameter to treat the self-interaction of the B-site cation's d-states, in order to determine the most appropriate method to study defect formation and the effect of spin on local structure. By calculating structural and electronic properties for different magnetic states we determine that $U = 4$ eV for Co in $LaCoO_3$ agrees best with available experiment. We demonstrate that the generalised gradient approximation (PBEsol+U) is most appropriate for studying structure versus spin state, while the local density approximation (LDA+U) is most appropriate to determine accurate energetics for defect properties.

PACS numbers: 71.15.Mb, 75.30.-m, 71.55.-i, 63.20.dk

I. INTRODUCTION

Solid oxide fuel cells (SOFCs) work by using catalytic processes to oxidise a variety of fuels at the anode while reducing oxygen at the cathode side, balanced by ion transport through the cell, thus generating electrical power with water as the waste product when H_2 is used as fuel.[1] They are a promising clean energy resource, but due to the chemical processes involved high temperatures are required for efficient operation.[2–6] For next-generation SOFCs, cathode layers that can conduct both ions and electrons at intermediate temperatures ($\sim$500$-$750° C), while remaining stable and compatible with the other layers in the cell, are required.[7–14] One of the most promising materials for such cathode layers is the $LaCoO_3$-based system $La_{1-x}Sr_xFe_{1-y}Co_yO_3$ (LSCF).[15–21] Finding the optimum doping concentrations for efficient fuel cell operation is, however, challenging, and input from computational modelling of the material properties in order to help formulate design improvements is crucial.[22]

Many computational techniques have been employed to study different aspects of SOFCs, from mesoscopic models[23–25] to interatomic potential-based methods[26–31] and *ab initio* calculations.[32–37] To understand the key properties of LSCF, such as defect formation, ionic conductivity, the mechanism of electronic conductivity, magnetic and electronic structure, and surface catalysis, requires an accurate but computationally tractable approach.[22,38–43] A fundamental requirement of such an approach is a sufficiently accurate description of the parent compound $LaCoO_3$.

At low temperatures, the perovskite $LaCoO_3$ stabilises in the rhombohedral phase ($R\bar{3}c$, no. 167).[44–46] As temperature T is varied, an interesting magnetic effect is observed. At low T (below $\sim$ 50 K) $LaCoO_3$ is a diamagnetic insulator.[47] As T is increased above 50 K, a pronounced spin-state transition occurs, where the system becomes a paramagnetic semiconductor, with another transition possibly occurring at $T > 500$ K, where the system becomes metallic.[47–49] Associated with the spin transitions are variations in the local structure and splittings in optical phonon modes, possibly indicating a Jahn-Teller distortion.[50–54] The nature of the spin transition has been extensively studied experimentally and computationally,[55–58] focussing on the d orbitals of the octahedrally coordinated Co ions, which are split by the crystal field. Initial proposals of a low spin (LS) to intermediate spin (IS) transition, possibly followed by a transition to high spin (HS),[48,59–63] have been superseded by more complicated scenarios involving different HS-LS orderings and possible defect-related effects to explain the experimental results.[64–70] Theoretical approaches applied include density functional theory (DFT),[71] using the local density approximation including a Hubbard U parameter (LDA+U),[60,72–75] dynamical mean-field theory,[69,76] and higher-level quantum chemical approaches.[61,77–80] Despite the sophistication of the methods applied, which become more computationally intense as complexity is increased, the nature of the spin state transition remains a topic of debate.[49,70,76,81–85]

To study defect properties, surface structure and catalysis, the most common approaches have been DFT (including Hubbard U)[86–90] and interatomic force field methods.[26,27,91–93] Such methods have been successful in modelling oxygen vacancy formation, ion migration, surface defect formation and oxygen reduction, but their application has not concerned the effect of local structure variations on macroscopic magnetic properties.

In this paper, we analyse simple DFT approaches to modelling the structural, magnetic, and electronic properties of $LaCoO_3$, in order to determine the optimum method to be used in studying the defect and catalytic properties of the material, as well as the magnetic effects on local structure. Our concern is to find the best method

that is both accurate and computationally tractable. We find that, for defect studies, LDA+U is most advantageous, while for local structure and magnetism the generalised gradient approximation with a Hubbard U parameter (GGA+U) is best from those surveyed. We find that a value of $U = 4$ eV is suitable in both cases. We demonstrate the applicability of our approaches by studying oxygen vacancy formation in the case of LDA+U, and studying phonon mode splitting and local structure modification as the spin state varies in the case of GGA+U. Our results serve as a guide to future computational studies of the spin and defect properties of $LaCoO_3$.

The paper is now structured as follows. In Sec. II we describe the DFT approaches used; in Sec. III we present our results, and in Sec. IV we summarise the main points of our study.

II. CALCULATIONS

We have used DFT to calculate the structural, electronic and magnetic properties of $LaCoO_3$ using a range of density functionals. All our DFT calculations were carried out using the `VASP` code,[94–97] utilizing the projector augmented wave (PAW) method[98] to model core and valence electron interactions (using the 'regular' PAW pseudopotential for O). The valence configurations used were: La ($5s^2 5p^6 6s^2 5d^1$), Co ($4s^2 3d^7$), O ($2s^2 2p^4$). To account for exchange and correlation, we have compared the LDA functional, the Perdew-Burke-Ernzerhof (PBE) GGA functional,[99] and the PBE functional corrected for solids (PBEsol),[100]. Moreover, the effect of adding a Hubbard U parameter (LDA+U, PBE+U, PBEsol+U) has been investigated, using the rotationally invariant approach of Dudarev *et al.*[101] As PBEsol was developed in order to reproduce lattice parameters more accurately than PBE,[100] one would expect improved structural properties over those found using other GGA approaches[86–88,102,103] (but less accurate cohesive energies). Furthermore, PBEsol is known to model well interatomic forces, resulting in accurate phonon frequencies.[36,104,105] Hybrid functionals, where a fraction of Hartree-Fock exact exchange is included,[106–108] were tested but we do not report any results here as we found that, as well as being prohibitively intensive computationally for larger systems, they represented the Co d states and material band gap in an erroneous manner, a result known from previous studies[109–111] on similar systems (we have included a comparison of our calculated structural properties using hybrid DFT with those of Gryaznov *et al.*,[112] see the Supplemental Material at [URL inserted by publisher]).

To avoid the problem of Pulay stress, the ion coordinates in the primitive rhombohedral cell (10 atoms) and the cell shape were optimised at constant volume for a series of different volumes, without enforcing symmetry constraints, and the resulting data fitted to the Murnaghan equation of state to determine the lowest energy structure. For IS and HS configurations relaxations were performed using the pseudocubic expansion of the primitive cell (40 atoms), which allows symmetry-breaking Jahn-Teller distortions to occur if favourable. The two cells are shown in Fig. 1. The plane-wave cut-off energy used was 650 eV and Brilloun zone sampling was performed, employing Gaussian smearing with a smearing width of 0.05 eV, on a 8×8×8 Monkhorst-Pack[113] k-point mesh for the primitive cell, and a 4×4×4 k-point mesh for the pseudocubic cell, which provided convergence in the total energy of up to 10^{-4} eV. Geometry optimisation was deemed to be converged when the interatomic forces were less than 10^{-2} eV/Å. For defect

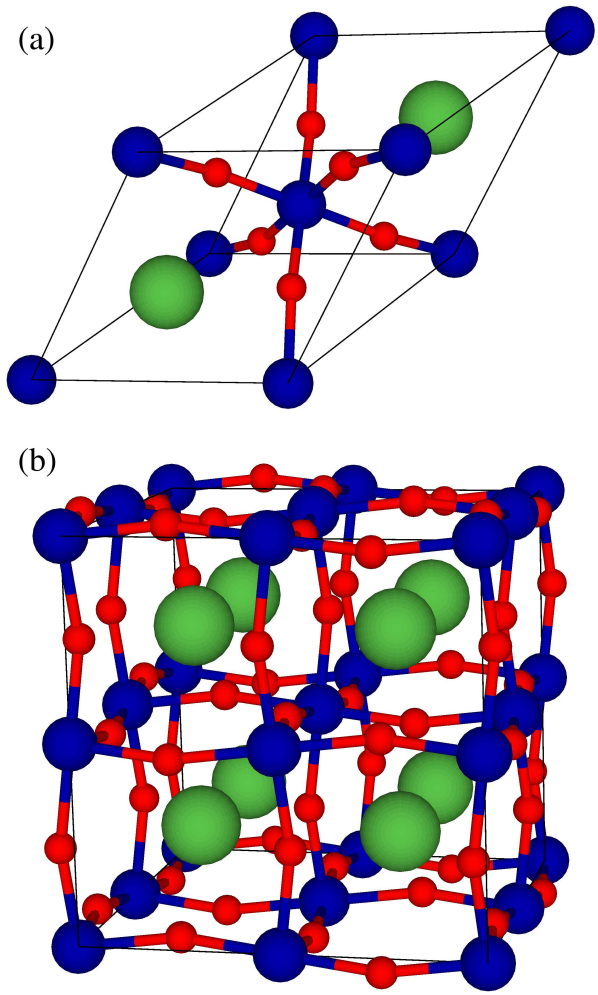

FIG. 1. (Color online) The unit cells of $LaCoO_3$ used in this work. (a) the 10 atom primitive rhombohedral cell. (b) The 40 atom pseudocubic expansion of the primitive cell. Where necessary, periodically repeated atoms are shown for clarity. La ions are represented by large light grey/green spheres, Co ions by intermediate-sized blue/darker grey spheres, and O ions by smaller red/dark grey spheres.

calculations, a 2×2×2 expansion of the pseudocubic cell, i.e. a 320 atom supercell, was used, with k-point sampling performed at the Γ point only. With this supercell the minimum distance between periodic images of point defects is 14.95 Å .

Phonon frequencies at the Γ point were determined using the frozen phonon approach, where the dynamical matrix is derived by displacing atoms from their equilibrium positions and calculating the resulting forces, thus giving the force constants. Atomic displacements of 0.01 Å were used and the convergence criterion for the self-consistent field iterative procedure was 10^{-7} eV. These force calculations were performed using the pseudocubic cell, the geometry of which had been relaxed so that the interatomic forces were less than 10^{-4} eV/Å , in order to determine accurate phonon frequencies. The dynamical matrix was diagonalised and the eigenvectors analysed using the post-processing program `PHONOPY`.[114]

The formation energy of a neutral oxygen vacancy, $E_f[V_{\rm O}^{\times}]$ (where we use the standard Kröger-Vink[115] notation), assuming thermodynamic equilibrium, was determined from the equation:

$$E_f[V_{\rm O}^{\times}] = E_{tot}[V_{\rm O}^{\times}] - E_{tot}[\text{bulk}] + \frac{1}{2}\mu_{\rm O_2}, \qquad (1)$$

where E_{tot}[bulk] is the total energy of the pure $LaCoO_3$ bulk supercell, $E_{tot}[V_{\rm O}^{\times}]$ is the total energy of the supercell containing a $V_{\rm O}^{\times}$, and $\mu_{\rm O_2}$ is the chemical potential of molecular oxygen. $\mu_{\rm O_2}$ has been determined using the standard approach in supercell DFT calculations.[116–119] We assume thermodynamical equilibrium with a reservoir of oxygen gas under oxygen-rich conditions, so that $\mu_{\rm O_2}$ is the energy of an O_2 molecule in the ground state (a triplet), i.e. excluding thermal contributions to the chemical potential.

III. RESULTS

TABLE I. Calculated rhombohedral lattice parameter (a) and angle (θ), determined using LDA, PBE, and PBEsol and compared with the low temperature neutron diffraction measurements from Ref. 44.

	a (Å)	θ (°)
Experiment	5.3416	60.99
LDA	5.2447	61.34
PBE	5.3613	61.20
PBEsol	5.2887	61.12

We first discuss our calculated lattice parameter (a) and rhombohedral angle (θ) of the ground state system using different density functionals, presented in Table I and Figure 2. As our simulations are at the athermal limit, we compare our results with the low temperature (4 K) neutron diffraction measurements of Thornton *et al.*[44] We find that the GGA and GGA+U functionals

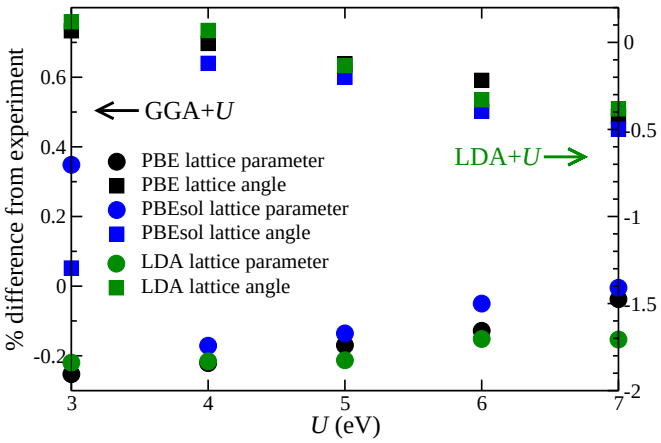

FIG. 2. (Color online) Percentage difference between the low temperature experimental[44] and the calculated rhombohedral lattice parameter (circles) and angle (squares), determined using LDA+U (shown in green/light grey), PBE+U (black), and PBEsol+U (blue/darker grey), shown as a function of U. The scale on the left ordinate axis corresponds to GGA+U, while that on the right corresponds to LDA+U).

give values in good agreement with the experimental results (with differences of less than 1%), while LDA and LDA+U underestimate the parameters by $\sim 2\%$. This underestimation is a well-known feature of LDA.[120]

We have calculated the electronic density of states (DOS) of $LaCoO_3$ (in the LS configuration) using different density functionals and present our results in Fig. 4, in comparison with the x-ray photoemission measurements of the upper valence band from Ref. 61. We summarise the calculated band gaps (LS state) in Table II, including $U = 4$ eV cases as representative examples of our DFT+U results (see the Supplemental Material at [URL inserted by publisher] for further data). The energy gap has been experimentally determined using photoemssion techniques to be 0.6 eV[121] and 0.9 eV,[122] and using optical conductivity measurements to be $0.1 - 1.0$ eV.[123–125] We find that LDA and GGA result in a metallic system, as expected due to the well-known self-interaction error and resulting band-gap underestimation that is a feature of these functionals. Adding a Hubbard U allows one to open a gap, which may be tuned by varying U (although one can derive a U parameter from first principles, as was done in Refs. 75 and 86). From Fig. 4 it is evident that varying U also varies the valence band width, indicating that there is a trade-off between these two properties, which must be balanced when choosing an appropriate U value.

In $LaCoO_3$, the Co cations are octahedrally coordinated with a formal oxidation state of 3+, meaning that the six d electrons can occupy the e_g and t_{2g} orbitals in the configurations shown in Fig. 3; that is in LS, IS or HS states. Moreover, the spin states can have ferromagnetic (FM) or antiferromagnetic (AFM) ordering amongst the

TABLE II. The energy band gap (in eV) and ground state spin configuration of $LaCoO_3$ as determined using different density functionals and compared with experimental results. 'Metal' indicates zero gap. For brevity the $U = 4$ eV cases are included as representative of the DFT+U functionals. In each case the band gap is calculated for the LS state (see text for the meanings of the acronyms used for spin states).

	Experiment	LDA	PBE	PBEsol	LDA+U	PBE+U	PBEsol+U
Band gap (eV)	0.6,[121] 0.9,[122] 0.1−1.1[123–125]	Metal	Metal	Metal	0.888	0.953	1.023
Spin state	LS	LS	LS	LS	LS	IS-HS FM	IS-HS FM

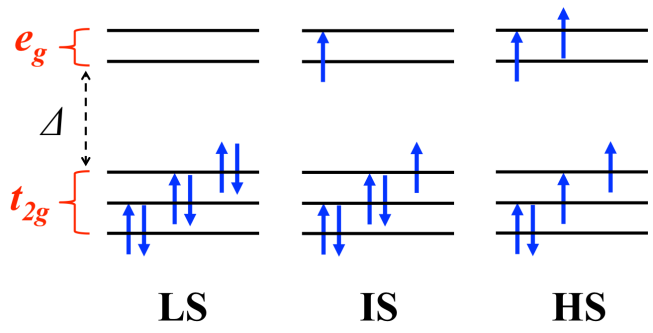

FIG. 3. (Color online) Schematic of the idealised spin states on the octahedrally coordinated Co cations in $LaCoO_3$: low spin (LS), intermediate spin (IS), and high spin (HS). The d states are split in energy (Δ) by the crystal field into e_g and t_{2g} orbitals. Upwards pointing arrows represent spin up electrons, downwards pointing represent spin down.

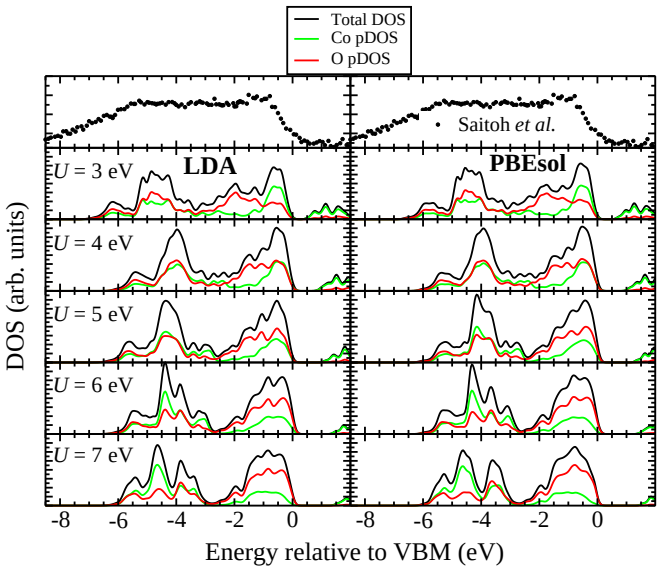

FIG. 4. (Color online) Calculated density of states (DOS) (black lines) and partial DOS (pDOS) (Co pDOS - light grey/green lines, O pDOS - dark grey/red lines) of $LaCoO_3$ determined using LDA+U and PBEsol+U, for different values of U. The energy scale is with respect to the valence band maximum (VBM). For comparison the x-ray photoemission results of Saitoh *et al.*[61] are shown (black dots).

Co-centred octahedra in different combinations, while it is also possible that there is ordered mixing of the LS, IS, and HS states. Which configuration is most favourable can be determined by calculating and comparing the total energies of the different spin combinations. We have performed such calculations to determine the ground state configuration for each density functional considered in this study. Our results are presented in Table II (see the Supplemental Material at [URL inserted by publisher] for further data). We find that LDA, GGA, and LDA+U result in a LS ground state configuration, which agrees with experiment as our simulations are at the athermal limit and $LaCoO_3$ is a diamagnetic insulator at low T. PBE+U and PBEsol+U result in an interesting ordered HS-IS FM configuration as the ground state, a point to which we return below.

To summarise the results presented so far, amongst the density functionals studied: for structural properties, GGA functionals give the most accurate results; for electronic properties LDA+U and GGA+U are most accurate; and for magnetic properties LDA, GGA and LDA+U are most accurate. Unsurprisingly, no simple DFT approach can accurately reproduce all these properties of $LaCoO_3$. Nevertheless, progress can be made by using LDA+U and PBEsol+U, as we demonstrate below. With LDA+U, well reproduced electronic and magnetic structure is gained at the expense of slightly underestimated structural parameters. For defect calculations and studies of surface catalysis, the reproduction of accurate energetics are required, while errors introduced by underestimated structural parameters should largely cancel, meaning that LDA+U will be a suitable functional for such studies. We note that this approach has been studied previously,[86] but was deemed inappropriate for oxygen vacancy formation calculations due to the calculated energy being higher than that determined experimentally, a point to which we return below. We find that PBEsol+U reproduces the structural parameters in excellent agreement with experiment, while also providing accurate electronic energies (although, as shown in Fig. 2, PBE+U also results in accurate structural properties, using PBEsol is known to model well interatomic forces[36,104,105] which are key for phonon frequency calculations). The calculated magnetic structures, however, involve mixtures of LS, IS and HS all close in energy (the ground state being ordered IS-HS FM). The differ-

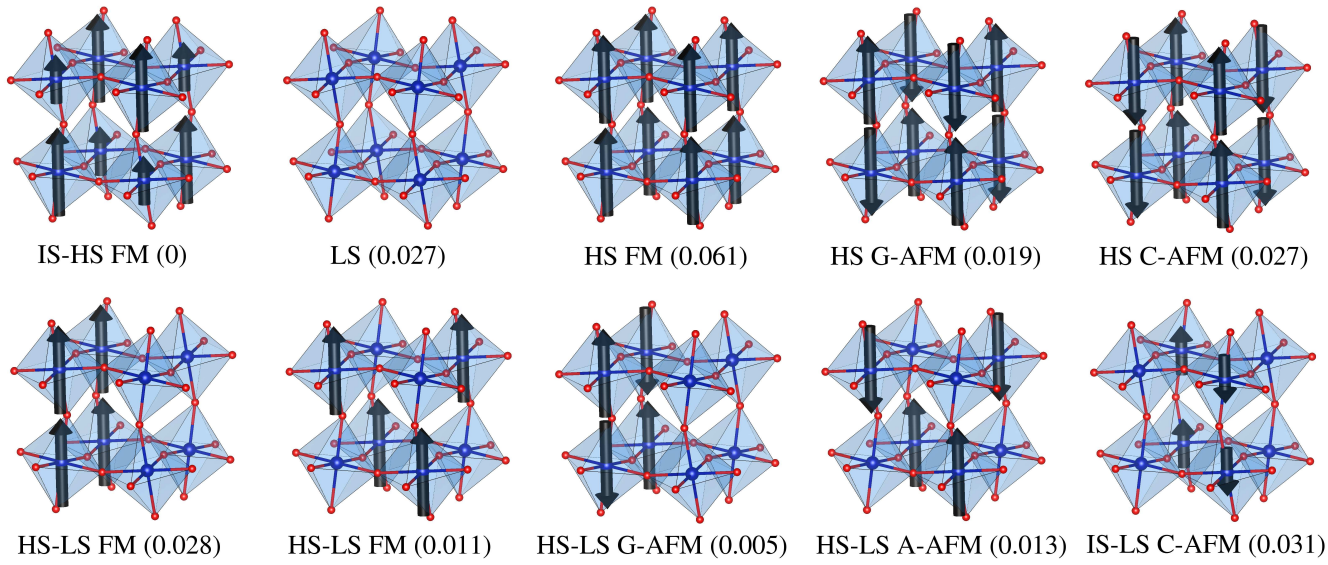

FIG. 5. (Color online) Schematic of the different spin configurations that are close in energy when using the PBEsol+U functional. The different states are combinations of low spin (LS), intermediate spin (IS), and high spin (HS) configurations with ferromagnetic (FM) or antiferromagnetic (AFM) ordering. AFM ordering can be of A-, C- or G-type. The numbers in parantheses are the energy differences per atom (in eV) between the spin configuration shown and the ground state (IS-HS FM). Spins are indicated by black arrows, the relative length of which distinguish between HS and IS. Co-centred polyhedra are shown, with blue spheres for Co and red for O. For clarity, La ions are not shown.

ent structures are shown in Fig. 5, where the standard notation to distinguish different types of AFM ordering (A-, C- and G-AFM) is used. For the HS-LS mixtures we find either layers that alternate along the [100] direction or channels of HS (with FM or AFM ordering) along [$\bar{1}$01], while for the IS-LS mixture we find alternating channels along [001]. The ground state IS-HS mix consists of alternating channels of each type along [$\bar{1}$01]. For pure HS A-AFM could not be stabilised. The accurate structural properties, coupled with the different magnetic structures lying close in energy, mean that this functional may be useful in studying local structural changes *vs* spin state. Considering the electronic DOS shown in Fig. 4, we see that in varying the U parameter there is a trade off between the energy band gap and the valence band width, as mentioned above. Setting $U = 4$ eV offers a good compromise in this trade off for both LDA+U and PBEsol+U. This value agrees well with that used in previous studies.[72,86] We also note from Fig. 2 that a higher value of U would result in slightly more accurate structural properties. The improvement in the percentage difference from experiment between $U = 4$ and e.g. $U = 7$, however, is less than 0.4 %, which would not be a significant improvement given the drastically worse electronic properties obtained with $U = 7$. $U = 4$ offers the best compromise for electronic and structural properties (moreover, LS is no longer the ground state for LDA+U with $U = 7$ eV, see the Supplemental Material at [URL inserted by publisher]).

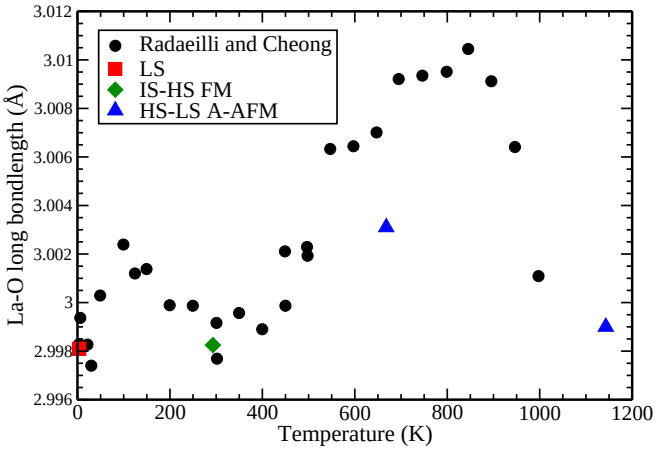

FIG. 6. (Color online) La-O long bond length calculated at different volumes, corresponding to different temperatures, for the spin transition LS to IS-HS FM to HS-LS A-AFM (red square, green diamond and blue triangles respectively), compared with neutron diffraction measurements from Ref. 53 (black circles).

To demonstrate the effectiveness of the PBEsol+U ($U = 4$ eV) density functional for studying the relationship between local structure and spin state, we have calculated, using the pseudocubic cell, the average La-O long bond length for the range of spin states shown in

Fig. 5 at T=4, 273, 668 and 1143 K in order to compare with the neutron diffraction measurements of Radaelli and Cheong.[53] To simulate the different temperatures, we have fixed the lattice parameters to those determined experimentally by Thornton *et al.*[44] and allow the internal ionic coordinates to relax. If we fix the low T bond length to that of Radeilli and Cheong,[53] and analyse the differences in calculated bond length as the spin state is varied, we find that the transition from LS (at $T = 4$ K) to the IS-HS FM state (occuring between $T = 4$ and $T = 273$ K), followed by a transition to the HS-LS A-AFM state (at $T > 273$ K) reproduces the experimental trend well (see Fig. 6). Such a spin transition is consistent with experimental studies, where strong evidence is found of HS states after the initial transition at $T > 50$ K, rather than just IS spin states.[64–70] We can conclude then that the PBEsol+U approach can indeed be used successfully for such structural *vs* spin state studies.

As a further example, we have calculated the zone-centre phonon modes of $LaCoO_3$ in different spin configurations, using PBEsol+U, in order to compare with the infrared (IR) measurements of Yamaguchi *et al.*[52] At low T (and hence the LS configuration), we calculate the IR stretching mode doublet to be 68 meV, in excellent agreement with experiment. Considering the transition to IS-HS FM ordering (see above), we find that the mode splits to 67 and 73 meV, again in excellent agreement with experiment.[52] (The associated phonon density of states are given in the Supplemental Material at [URL inserted by publisher]). This result further reinforces our conclusion that we can use this approach to study local structure *vs* spin state. Indeed, we find that, if we were to used LDA+U instead, the calculated low-T IR streching mode doublet is 73 meV, an overestimation of ~ 7 %. As using LDA+U results in underestimated lattice parameters (see Fig. 2), this increase in the calculated frequency is unsurprising.

Using LDA+U, we have calculated the formation energy of an oxygen vacancy to be 3.36 eV, with AFM ordering on the neighbouring reduced Co ions. The calculated magnetic moment $\mu = 1.6\mu_B$. This result is in good agreement with previous computational studies in the literature using a variety of theoretical approaches.[33,86,87,92] It is, however, significantly higher than the value of 2.2 eV determined experimentally,[126] but, given the low levels of non-stoichiometry observed in undoped $LaCoO_{3-\delta}$ ($\delta \leq 0.01$),[126] comparison with this value should take into account that vacancies on the surface may play a significant role in the reduction process. The surface vacancy formation energy has been determined to be lower than in the bulk by $\sim 1-2$ eV[87,93] (this effect has also been determined in the related perovskite perovskite $LaMnO_3$[40]). Such a result demonstrates that the LDA+U approach can be used for studies of defect properties of this material. If instead we employ the PBEsol+U functional, we immdediately have the problem that the ground state spin configuration of the defect-free system is not LS. When forming a defect, many spin configurations can be converged, and choosing the most appropriate one is difficult given that the original configuration is incorrect. Using the lowest total energy results, we calculate a formation energy of 6.14 eV, a value that is substantially higher than that determined using LDA+U and inconsistent with experimental results. Similar problems are expected when using PBE+U, as the ground state spin configuration is also not LS in that case. These complications, which both lead to results that are most likely not comparable with experiment and increase the computational load (due to the necessity of checking the many different possible configurations), lead us to conclude that GGA+U is drastically less favourable than LDA+U when studying defects.

IV. SUMMARY/CONCLUSIONS

In summary, we have compared the results of calculated electronic, structural and magnetic properties of $LaCoO_3$ using a range of standard density functionals in order to determine the optimum DFT approach to study local distortions and defect formation. We found that no single DFT approach could model simultaneously all these aspects accurately, but that two clear approaches, LDA+U and PBEsol+U, offered the most advantages for defect properties and structural studies *vs* spin states, respectively. We found that in both cases $U = 4$ eV gave results in good agreement with experiment. We demonstrated the applicability of these approaches by calculating the formation energy of an oxygen vacancy using LDA+U, finding excellent agreement with previous studies in the literature, and by determining the local structural variation and phonon mode splitting for different spin configurations, finding that the transition from LS to ordered HS-IS to HS resulted in good agreement with experiment. Our results demonstrate that simple DFT methods can be used to study complex features of $LaCoO_3$.

ACKNOWLEDGMENT

The authors acknowledge funding from EPSRC grant EP/K016288/1. The authors also acknowledge the use of the UCL Legion High Performance Computing Facility (Legion@UCL) and associated support services, the IRIDIS cluster provided by the EPSRC funded Centre for Innovation (EP/K000144/1 and EP/K000136/1), and the ARCHER supercomputer through membership of the UK's HPC Materials Chemistry Consortium, which is funded by EPSRC grant EP/L000202, in the completion of this work.

* j.buckeridge@ucl.ac.uk

[1] S. C. Singhal and K. Kendall, in *High Temperature and Solid Oxide Fuel Cells*, ed. S. C. Singhal and K. Kendal, Elsevier Science, Amsterdam, 2003, pp. 1 – 22.
[2] S. C. Singhal, Solid State Ionics **135**, 305 (2000).
[3] R. M. Ormerod, Chem. Soc. Rev. **32**, 17 (2003).
[4] S. P. S. Badwal, Solid State Ionics **143**, 39 (2001).
[5] A. B. Stambouli and E. Traversa, Renew. Sust. Ener. Rev. **6**, 433 (2002).
[6] A. Lashtabeg and S. J. Skinner, J. Mater. Chem. **16**, 3161 (2006).
[7] B. C. H. Steele and A. Heinzel, Nature **414**, 345 (2001).
[8] A. Weber and E. Ivers-Tiffée, J. Power Sources **127**, 273 (2004).
[9] F. Tietz, Ionics **5**, 129 (1999).
[10] . S. Aricò, P. Bruce, B. Scrosati, J.-M. Tarascon and W. van Schalkwijk, Nature Mater. **4**, 366 (2005).
[11] E. D. Wachsman and K. T. Lee, Science **334**, 935 (2011).
[12] Z. Shao and S. M. Haile, Nature **431**, 170 (2004).
[13] A. Tarancón, M. Burriel, J. Santiso, S. J. Skinner and J. A. Kilner, J. Mater. Chem. **20**, 3799 (2010).
[14] J. M. Vohs and R. J. Gorte, Adv. Mater. **21**, 943 (2009).
[15] V. Dusastre and J. A. Kilner, Solid State Ionics **126**, 163 (1999).
[16] S. M. Haile, Acta Mater. **51**, 5981 (2003).
[17] A. Aguadero, L. Fawcett, S. Taub, R. Woolley, K.-T. Wu, N. Xu, J. A. Kilner and S. J. Skinner, J. Mater. Sci. **47**, 3925 (2012).
[18] E. Ivers-Tiffée, A. Weber and D. Herbstritt, J. Eur. Ceram. Soc. **21**, 1805 (2001).
[19] D. J. L. Brett, A. Atkinson, N. P. Brandon and S. J. Skinner, Chem. Soc. Rev. **37**, 1568 (2008).
[20] H. Ullmann, N. Trofimenko, F. Tietz, D. Stöver and A. Ahmad-Khanlou, Solid State Ionics **138**, 79 (2000).
[21] S. J. Skinner, Int. J. Inorg. Mater. **3**, 113 (2001).
[22] M. Liu, M. E. Lynch, K. Blinn, F. M. Alamgir and Y. Choi, Materials Today **14**, 534 (2011).
[23] M. Liu, J. Electrochem. Soc. **145**, 142 (1998).
[24] J. E. Saal, *Ph.D. thesis*, The Pennsylvania State University, 2010.
[25] J. E. Saal, Y. Wang, S. Shang and Z.-K. Liu, Inorg. Chem. **49**, 10291 (2010).
[26] M. S. Islam, M. Cherry and C. R. A. Catlow, J. Solid State Chem. **124**, 230 (1996).
[27] M. Saiful Islam, J. Mater. Chem. **10**, 1027 (2000).
[28] S. M. Woodley, J. D. Gale, P. D. Battle and C. R. A. Catlow, J. Chem. Phys. **119**, 9737 (2003).
[29] A. Jones, and M. S. Islam, J. Phys. Chem. C **112**, 4455 (2008).
[30] A. Chroneos, B. Yildiz, A. Tarancon, D. Parfitt and J. A. Kilner, Energy Environ. Sci. **4**, 2774 (2011).
[31] D. S. D. Gunn, N. L. Allan and J. A. Purton, J. Mater. Chem. A **2**, 13407 (2014).
[32] A. B. Muñoz Garcìa, A. M. Ritzmann, M. Pavone, J. A. Keith and E. A. Carter, Acc. Chem. Res. **47**, 3340 (2014).
[33] M. Pavone, A. M. Ritzmann and E. A. Carter, Energy Environ. Sci. **4**, 4933 (2011).
[34] A. M. Ritzmann, A. B. Muñoz Garcìa, M. Pavone, J. A. Keith and E. A. Carter, MRS Commun. **3**, 161 (2013).
[35] H.-T. Chen, P. Raghunath and M. C. Lin, Langmuir **27**, 6787 (2011).
[36] J. Buckeridge, D. O. Scanlon, A. Walsh, C. R. A. Catlow and A. A. Sokol, Phys. Rev. B **87**, 214304 (2013).
[37] X. Aparicio-Anglès, A. Roldan and N. H. de Leeuw, Chem. Mater. **27**, 7910 (2015).
[38] J. Suntivich, H. A. Gasteiger, N. Yabuuchi, H. Nakanishi, J. B. Goodenough and Y. Shao-Horn, Nature Chemistry **3**, 546 (2011).
[39] Y. A. Mastrikov, R. Merkle, E. Heifets, E. A. Kotomin and J. Maier, J. Phys. Chem. C **114**, 3017 (2010).
[40] S. Piskunov, T. Jacob and E. Spohr, Phys. Rev. B **83**, 073402 (2011).
[41] D. Fuks, A. Weizman and E. Kotomin, Phys. Stat. Sol. b **250**, 864 (2013).
[42] A. M. Ritzmann, A. B. Muñoz García, M. Pavone, J. A. Keith and E. A. Carter, Chem. Mater. **25**, 3011 (2013).
[43] V. M. Tapilin, A. R. Cholach and N. N. Bulgakov, J. Phys. Chem. Sol. **71**, 1581 (2010).
[44] G. Thornton, B. Tofield and A. Hewat, J. Solid State Chem. **61**, 301 (1986).
[45] V. Øygarden, H. L. Lein and T. Grande, J. Solid State Chem. **192**, 246 (2012).
[46] C. Autret, J. Hejtmánek, K. Knížek, M. Maryško, Z. Jirák, M. Dlouhá and S. Vratislav, J. Phys.: Condens. Matter **17**, 1601 (2005).
[47] K. Asai, A. Yoneda, O. Yokokura, J. Tranquada, G. Shirane and K. Kohn, J. Phys. Soc. Jpn. **67**, 290 (1998).
[48] C. Zobel, M. Kriener, D. Bruns, J. Baier, M. Grüninger, T. Lorenz, P. Reutler and A. Revcolevschi, Phys. Rev. B **66**, 020402 (2002).
[49] A. Gulec and R. F. Klie, J. Appl. Phys. **116**, 233701 (2014).
[50] O. Haas, R. P. W. J. Struis and J. M. McBreen, J. Solid State Chem. **177**, 1000 (2004).
[51] G. Maris, Y. Ren, V. Volotchaev, C. Zobel, T. Lorenz and T. T. M. Palstra, Phys. Rev. B **67**, 224423 (2003).
[52] S. Yamaguchi, Y. Okimoto and Y. Tokura, Phys. Rev. B **55**, R8666 (1997).
[53] P. G. Radaelli and S.-W. Cheong, Phys. Rev. B **66**, 094408 (2002).
[54] A. Ishikawa, J. Nohara and S. Sugai, Phys. Rev. Lett. **93**, 136401 (2004).
[55] S. Stølen, F. Grønvold, H. Brinks, T. Atake and H. Mori, Phys. Rev. B **55**, 14103 (1997).
[56] H. R. Aliabad, V. Hesam, I. Ahmad and I. Khan, Physica B **410**, 112 (2013).
[57] S. K. Pandey, A. Kumar, S. Patil, V. R. R. Medicherla, R. S. Singh, K. Maiti, D. Prabhakaran, A. T. Boothroyd and A. V. Pimpale, Phys. Rev. B **77**, 045123 (2008).
[58] W. T. Hong, M. Gadre, Y.-L. Lee, M. D. Biegalski, H. M. Christen, D. Morgan and Y. Shao-Horn, J. Phys. Chem. Lett. **4**, 2493 (2013).
[59] M. Abbate, J. C. Fuggle, A. Fujimori, L. H. Tjeng, C. T. Chen, R. Potze, G. A. Sawatzky, H. Eisaki and S. Uchida, Phys. Rev. B **47**, 16124 (1993).
[60] M. A. Korotin, S. Y. Ezhov, I. V. Solovyev, V. I. Anisimov, D. I. Khomskii and G. A. Sawatzky, Phys. Rev. B **54**, 5309 (1996).
[61] T. Saitoh, T. Mizokawa, A. Fujimori, M. Abbate, Y. Takeda and M. Takano, Phys. Rev. B **55**, 4257 (1997).
[62] D. Louca, J. L. Sarrao, J. D. Thompson, H. Röder and G. H. Kwei, Phys. Rev. B **60**, 10378 (1999).

[63] Y. Kobayashi, T. S. Naing, M. Suzuki, M. Akimitsu, K. Asai, K. Yamada, J. Akimitsu, P. Manuel, J. M. Tranquada and G. Shirane, Phys. Rev. B **72**, 174405 (2005).

[64] A. Podlesnyak, S. Streule, J. Mesot, M. Medarde, E. Pomjakushina, K. Conder, A. Tanaka, M. W. Haverkort and D. I. Khomskii, Phys. Rev. Lett. **97**, 247208 (2006).

[65] M. W. Haverkort, Z. Hu, J. C. Cezar, T. Burnus, H. Hartmann, M. Reuther, C. Zobel, T. Lorenz, A. Tanaka, N. B. Brookes, H. H. Hsieh, H.-J. Lin, C. T. Chen and L. H. Tjeng, Phys. Rev. Lett. **97**, 176405 (2006).

[66] R. Schmidt, J. Wu, C. Leighton and I. Terry, Phys. Rev. B **79**, 125105 (2009).

[67] S. Medling, Y. Lee, H. Zheng, J. F. Mitchell, J. W. Freeland, B. N. Harmon and F. Bridges, Phys. Rev. Lett. **109**, 157204 (2012).

[68] S. Ovchinnikov, Y. Orlov and V. Dudnikov, J. Magn. Magn. Mater. **324**, 3584 (2012).

[69] V. Křápek, P. Novák, J. Kuneš, D. Novoselov, D. M. Korotin and V. I. Anisimov, Phys. Rev. B **86**, 195104 (2012).

[70] S. El-Khatib, D. Phelan, J. G. Barker, H. Zheng, J. F. Mitchell and C. Leighton, Phys. Rev. B **92**, 060404 (2015).

[71] P. Ravindran, P. A. Korzhavyi, H. Fjellvåg and A. Kjekshus, Phys. Rev. B **60**, 16423 (1999).

[72] M. Abbate, R. Potze, G. A. Sawatzky and A. Fujimori, Phys. Rev. B **49**, 7210 (1994).

[73] M. Sahnoun, C. Daul, O. Haas and A. Wokaun, J. Phys.: Condens. Matter **17**, 7995 (2005).

[74] A. Laref and S. J. Luo, J. Phys. Soc. Jpn. **79**, 064702 (2010).

[75] H. Hsu, K. Umemoto, M. Cococcioni and R. Wentzcovitch, Phys. Rev. B **79**, 125124 (2009).

[76] M. Izquierdo, M. Karolak, C. Trabant, K. Holldack, A. Föhlisch, K. Kummer, D. Prabhakaran, A. T. Boothroyd, M. Spiwek, A. Belozerov, A. Poteryaev, A. Lichtenstein and S. L. Molodtsov, Phys. Rev. B **90**, 235128 (2014).

[77] H. Takahashi, F. Munakata and M. Yamanaka, Phys. Rev. B **57**, 15211 (1998).

[78] R. Eder, Phys. Rev. B **81**, 035101 (2010).

[79] L. Siurakshina, B. Paulus, V. Yushankhai and E. Sivachenko, Eur. Phys. J. B **74**, 53 (2010).

[80] Y. Wang, Z. Wang, Z. Fang and X. Dai, Phys. Rev. B **91**, 125139 (2015).

[81] A. M. Durand, D. P. Belanger, C. H. Booth, F. Ye, S. Chi, J. A. Fernandez-Baca and M. Bhat, J. Phys.: Condens. Matter **25**, 382203 (2013).

[82] A. M. Durand, D. P. Belanger, T. J. Hamil, F. Ye, S. Chi, J. A. Fernandez-Baca, C. H. Booth, Y. Abdollahian and M. Bhat, J. Phys.: Condens. Matter **27**, 176003 (2015).

[83] J.-H. Kwon, W. S. Choi, Y.-K. Kwon, R. Jung, J.-M. Zuo, H. N. Lee and M. Kim, Chem. Mater. **26**, 2496 (2014).

[84] J. Fujioka, Y. Yamasaki, A. Doi, H. Nakao, R. Kumai, Y. Murakami, M. Nakamura, M. Kawasaki, T. Arima and Y. Tokura, Phys. Rev. B **92**, 195115 (2015).

[85] D. P. Belanger, T. Keiber, F. Bridges, A. M. Durand, A. Mehta, H. Zheng, J. F. Mitchell and V. Borzenets, J. Phys.: Condens. Matter **28**, 025602 (2016).

[86] A. M. Ritzmann, M. Pavone, A. B. Muñoz Garcìa, J. A. Keith and E. A. Carter, J. Mater. Chem. A **2**, 8060 (2014).

[87] A. Kushima, S. Yip and B. Yildiz, Phys. Rev. B **82**, 115435 (2010).

[88] J. W. Han and B. Yildiz, J. Mater. Chem. **21**, 18983 (2011).

[89] S. O. Choi, M. Penninger, C. H. Kim, W. F. Schneider and L. T. Thompson, ACS Catal. **3**, 2719 (2013).

[90] X. Cheng, E. Fabbri, M. Nachtegaal, I. E. Castelli, M. E. Kazzi, R. Haumont, N. Marzari and T. J. Schmidt, Chem. Mater. **27**, 7662 (2015).

[91] M. Cherry, M. S. Islam and C. R. A. Catlow, J. Solid State Chem. **118**, 125 (1995).

[92] M. S. D. Read, M. Saiful Islam, G. W. Watson, F. King and F. E. Hancock, J. Mater. Chem. **10**, 2298 (2000).

[93] S. Khan, R. J. Oldman, F. Cora, C. R. A. Catlow, S. A. French and S. A. Axon, Phys. Chem. Chem. Phys. **8**, 5207 (2006).

[94] G. Kresse and J. Hafner, Phys. Rev. B **47**, 558 (1993).

[95] G. Kresse and J. Hafner, Phys. Rev. B **49**, 14251 (1994).

[96] G. Kresse and J. Furthmüller, Comput. Mater. Sci. **6**, 15 (1996).

[97] G. Kresse and J. Furthmüller, Phys. Rev. B **54**, 11169 (1996).

[98] P. E. Blöchl, Phys. Rev. B **50**, 17953 (1994).

[99] J. P. Perdew, K. Burke and M. Ernzerhof, Phys. Rev. Lett. **77**, 3865 (1996).

[100] J. P. Perdew, A. Ruzsinszky, G. I. Csonka, O. A. Vydrov, G. E. Scuseria, L. A. Constantin, X. Zhou and K. Burke, Phys. Rev. Lett. **100**, 136406 (2008).

[101] S. L. Dudarev, G. A. Botton, S. Y. Savrasov, C. J. Humphreys and A. P. Sutton, Phys. Rev. B **57**, 1505 (1998).

[102] K. Knížek, Z. Jirák, J. Hejtmánek and P. Novák, J. Phys.: Condens. Matter **18**, 3285 (2006).

[103] K. Knížek, Z. c. v. Jirák, J. c. v. Hejtmánek, P. Novák and W. Ku, Phys. Rev. B **79**, 014430 (2009).

[104] J. M. Skelton, S. C. Parker, A. Togo, I. Tanaka and A. Walsh, Phys. Rev. B **89**, 205203 (2014).

[105] J. Buckeridge, D. O. Scanlon, T. D. Veal, M. J. Ashwin, A. Walsh and C. R. A. Catlow, Phys. Rev. B **89**, 014107 (2014).

[106] M. Ernzerhof and G. E. Scuseria, J. Chem. Phys. **110**, 5029 (1999).

[107] J. Heyd, G. E. Scuseria and M. Ernzerhof, J. Chem. Phys. **118**, 8207 (2003).

[108] J. Heyd, G. E. Scuseria and M. Ernzerhof, J. Chem. Phys. **124**, 219906 (2006).

[109] K. G. Godinho, J. J. Carey, B. J. Morgan, D. O. Scanlon and G. W. Watson, J. Mater. Chem. **20**, 1086 (2010).

[110] D. O. Scanlon and G. W. Watson, Phys. Chem. Chem. Phys. **13**, 9667 (2011).

[111] D. O. Scanlon and G. W. Watson, J. Mater. Chem. **21**, 3655 (2011).

[112] D. Gryaznov, R. A. Evarestov and J. Maier, Phys. Rev. B **82**, 224301 (2010).

[113] H. J. Monkhorst and J. D. Pack, Phys. Rev. B **13**, 5188 (1976).

[114] A. Togo, F. Oba and I. Tanaka, Phys. Rev. B **78**, 134106 (2008).

[115] F. A. Kröger and H. J. Vink, in *Solid State Physics*, Academic Press, vol. **3**, pp. 307–435 1956.

[116] C. G. V. de Walle and J. Neugebauer, J. Appl. Phys. **95**, 3851 (2004).

[117] C. Persson, Y.-J. Zhao, S. Lany and A. Zunger, Phys. Rev. B **72**, 035211 (2005).

[118] J. Buckeridge, D. O. Scanlon, A. Walsh and C. R. A. Catlow, Comput. Phys. Commun. **185**, 330 (2014).

[119] D. O. Scanlon, J. Buckeridge, C. R. A. Catlow and G. W. Watson, J. Mater. Chem. C **2**, 3429 (2014).

[120] A. van de Walle and G. Ceder, Phys. Rev. B **59**, 14992 (1999).
[121] A. Chainani, M. Mathew and D. D. Sarma, Phys. Rev. B **46**, 9976 (1992).
[122] M. Abbate, J. C. Fuggle, A. Fujimori, L. H. Tjeng, C. T. Chen, R. Potze, G. A. Sawatzky, H. Eisaki and S. Uchida, Phys. Rev. B **47**, 16124 (1993).
[123] T. Arima, Y. Tokura and J. B. Torrance, Phys. Rev. B **48**, 17006 (1993).
[124] Y. Tokura, Y. Okimoto, S. Yamaguchi, H. Taniguchi, T. Kimura and H. Takagi, Phys. Rev. B **58**, R1699 (1998).
[125] A. R. Sarker, Int. J. Mater. Sci. Appl. **4**, 159 (2015).
[126] J. Mizusaki, Y. Mima, S. Yamauchi, K. Fueki and H. Tagawa, J. Solid State Chem. **80**, 102 (1989).